Monocyte-derived alveolar macrophages mediate resistance to migrating helminths through depletion of arginine availability

Fei Chen[1,2], Darine W. El Naccache[1,2,3], John Ponessa[1,2,3], Alexander Lemenze[1,4], Vanessa Espinosa[1,5], Wenhui Wu[1,2], Katherine Lothstein[1,2], Linhua Jin[1,2], Amariliz Rivera[1,5], Mark Siracusa[1,2,6], and William C. Gause[1,2,6]

[1]Center for Immunity and Inflammation, [2]Department of Medicine, [4]Department of Pathology, Immunology, and Laboratory Medicine, and [5]Department of Pediatrics, New Jersey Medical School, Rutgers—The State University of New Jersey, Newark, New Jersey, USA.
[3]Authors contributed equally
[6]Authors contributed equally

Abstract
We examined the activation and effector functions of lung macrophages in mediating immunity against helminth parasites. Using fate mapping mice, we showed that monocytes recruited to the lung assume an alveolar macrophage phenotype and comprise as many as 10% of alveolar macrophages by 7 days after inoculation. Monocyte-derived alveolar macrophages assume distinct transcriptional and metabolic profiles that include high levels of arginase expression and preferentially mediate helminth damage, both of which are dependent on neutrophil help. In further studies, arginase was shown to mediate helminth killing through localized depletion of arginine.

Introduction:

Helminth infections trigger potent type 2 immune responses characterized by elevations in IL-4, IL-5, and IL-13. This response can mediate host protection through limiting parasite burden and by mitigating tissue damage associated with trafficking of these large multicellular parasites through host tissues[1]. Although helminth infections continue to be a major global health problem, as yet effective vaccines have been elusive, likely in part because cellular and molecular mechanisms through which the type 2 immune response mediates resistance remain unclear. A critical stage of the life cycle of many helminths, including intestinal nematode parasites, involves passage through the lung. Previous studies have indicated that the lung plays a significant role in early parasite clearance and as such is a potential target for vaccine-induced acquired resistance [2,3].

Both innate and adaptive components of the type 2 immune response likely contribute to resistance. IL-4Rα signaling is required for the activation of a diverse population of distinct innate immune cell lineages, including innate lymphoid type 2 cells and myeloid cells, as well as antigen-specific T and B cells. Various immune mediated resistance mechanisms include increased epithelial cell turnover, increased intestinal luminal fluid flow and muscle contractility, antibody-dependent mechanisms, production of mast cell-derived mediators, goblet cell secretion of mucous and other effector molecules, and eosinophil-mediated effector mechanisms. Recent studies further indicate that macrophages and neutrophils may also contribute to helminth resistance. Though classically associated with resistance to microbial pathogens, both

macrophages and neutrophils have now been shown to be differentially activated during helminth infections and to mediate potent resistance mechanisms[3-5]. Neutrophils not only directly target helminths[4], but can stimulate macrophages to assume an alternatively activated state required for their anti-helminth effector functions[3,6]. Recent studies indicate that macrophages primed by helminths in the intestine, lung and skin can mediate helminth killing both in vitro and in these tissue microenvironments[2,3,7-9].

An emerging body of literature now supports a model in which tissue-resident macrophage populations can be subdivided into tissue-derived macrophages (TD-macs) and monocyte-derived macrophages (Mo-macs). TD-macs develop during the early stages of fetal development from the yolk sac and fetal liver, and populate tissues under steady-state conditions, whereas Mo-macs develop from bone marrow-resident precursor cells and can enter tissues in the context of inflammation[10-13]. In the lung microenvironment, tissue derived alveolar macrophages (TD-AMs) mediate homeostasis through surfactant recycling and also provide surveillance for early recognition of pathogens invading the airways[14]. During infection monocytes are rapidly recruited to the lung, where they differentiate into macrophages. Recent studies suggest that monocytes can also differentiate into an alveolar macrophage-like phenotype and that these Mo-AM can function differently than TD-AMs[15]. In one study, the Mo-AMs were the predominate lung macrophage subset contributing to fibrosis in a bleomycin-induced lung injury model[16]. Despite these substantial advances, studies examining the development of Mo-AMs have primarily relied on radiation chimeras or other nonphysiological approaches raising questions as to the physiological significance of these observations. Further, whether Mo-AMs populate the lung and perform distinct functions in the context of helminth infections remains to be determined.

Although the anti-helminth qualities of macrophages are well-documented, there is a substantial knowledge gap regarding the mechanisms they employ to promote parasite killing. While not experimentally defined, studies have associated the anti-helminth properties of macrophages with activity of the enzyme arginase 1 (Arg1)[3,7,17]. Arg1 is known to mediate a cascade of effects leading to potentially toxic urea production and also polyamine synthesis which may contribute to immune cell activation and proliferation[17]. Arg1 can also mediate the localized depletion of arginine, which can have immunoregulatory effects on activated immune cells such as T cells[18]. However, whether any of these mechanisms or other potentially associated mechanisms are important in mediating macrophage killing of helminth parasites and whether they are distinctly initiated specific subsets of macrophages remains uncertain.

Infection with the intestinal nematode parasite, *N. brasiliensis* (Nb) is a well-established rodent experimental model showing a similar life cycle to human hookworms. Studies in this model have substantially advanced our understanding of inflammation and macrophage biology in the lung. Infective third-stage larvae (L3) migrate from the skin to the lung before entering the small intestine. The lung is an important site, at which both innate and adaptive components of the type 2 immune response interact with the migrating parasitic larval stages[2,5,19]. Previous studies have shown that CD4 T cell depletion at the time of secondary inoculation does not affect accelerated resistance, which is also intact in B cell deficient mice[20,21]. Lung macrophages primed by primary Nb inoculation have previously been shown to play an

important role in acquired resistance and highly purified helminth-primed lung macrophages can effectively kill L3 in vitro[3].

Here we used macrophage lineage fate mapping mice to investigate the role of lung macrophage subsets of different progenitor origins in mediating acquired resistance to Nb. We further elucidate the role of neutrophils in driving their effector function and for the first time revealed how macrophages mediate resistance against helminths.

Results:

Nb L3 enter the lung as early as 12 hours after subcutaneous inoculation. To examine how this parasite invasion of the lung affected levels of monocytes and macrophages, these populations were analyzed using flow cytometric analyses at days 1, 7, and 14 after inoculation. Marked increases in total number of macrophages were observed by day 7 after inoculation (**Fig. 1a**) while Ly6C^{+} monocytes were markedly increased within 24 hours, consistent with their rapid recruitment, peaked at day 7, and had dropped markedly by day 14 (**Fig. 1b**). Alveolar macrophages (AMs) (CD64+,F4/80+,SiglecF+, CD11c+) were slightly elevated as early as day 1 but showed marked increases, more than doubling by day 7 (**Fig. 1c**). Non alveolar macrophages (NAMs) (CD64+, F4/80+, SiglecF-, CD11c^{var}), primarily derived from recruited monocytes, were also markedly elevated by day 7 after Nb inoculation (**Fig. 1d**). In comparison, eosinophils, also associated with Nb infection, were not elevated until day 7 after inoculation and remained elevated at day 14 (**Fig. 1e**). Collectively, these data demonstrate that Nb promotes substantial changes in lung macrophage subsets.

Previous work has shown that by day 7 after Nb inoculation sort purified lung macrophages can effectively kill infectious Nb larvae (L3) following in vitro culture[3]. However, these lung macrophage populations are comprised of both AMs and NAMs. Whether these two macrophage subsets equally or preferentially contribute to parasite killing remains unknown. To test this, at day 7 after Nb inoculation, lung cell suspensions were prepared as previously described[3], and AMs and NAMs were sort purified. Individual macrophage subsets ($1X10^{6}$/ml) were then cultured with exsheathed L3 (100/well) in 24 well plates, for 5 days, as previously described with bulk macrophages[3]. As shown in **Fig. 2a**, AMs were approximately 5X more effective at killing L3 than NAMs. Assessment of parasite metabolic activity by assaying their ATP levels[3] further showed decreased activity in AMs compared to NAMs (**Fig. 2b**). Previous studies have shown that Arg1 production by macrophages is essential for effective killing of parasitic larvae both in vitro and in vivo[7,19]. Therefore, to investigate whether the macrophage killing observed correlated with Arg1 production, AMs and NAMs were assessed for cytoplasmic Arg1 expression at 7 days after Nb infection. As shown in **Fig. 2c**, more than 10% of AMs expressed Arg1 after infection, while less than 3% of NAMs from treated mice expressed Arg1. Furthermore, the total number of Arg1 expressing AMs was significantly greater than NAMs (**Fig. 2d**). Collectively, these studies strongly suggest that AMs mediate the majority of the parasite killing capacity within lung macrophage compartments and that elevated cytoplasmic Arg1 protein expression is associated with that enhanced capacity in a subset representing about 10% of AMs.

Our previous studies showed that transfer of bulk lung macrophages from Nb primed mice to naïve recipient mice was sufficient to mediate accelerated resistance similar to the memory response observed after secondary challenge[3]. To examine whether AMs also showed preferential resistance in vivo, AMs and NAMs were sort-purified from the lungs of donor mice at day 7 after Nb inoculation and transferred to naïve recipient mice, which were then inoculated with Nb. Unexpectedly, as shown in **Fig. 3a**, both AMs and NAMs were equally effective at mediating accelerated acquired resistance in recipient mice at 5 days after Nb inoculation. These studies suggested that either the NAMs were quite capable of killing parasites in vivo or alternatively that the transferred NAMs were differentiating into an AM-like subset that acquired the ability to preferentially kill invading parasitic larvae. To test whether an AM phenotype could develop in the lung from NAMs, we isolated AMs and NAMs from donor CD45.1 mice at day 7 after Nb inoculation and transferred these subsets intratracheally to naïve congenic CD45.2 recipients. Recipient mice were rested 2 days, inoculated with Nb and 5 days later lung cell suspensions were collected and assessed for donor and recipient AM populations. As shown in **Fig. 3b**, transferred CD45.1 donor NAMs gave rise to a substantial number of AMs comprising about 10% of the total AM population in the CD45.2 congenic recipients. To investigate effects of monocyte depletion on the AM population we obtained CCR2 GFP reporter and CCR2 Diptheria toxin receptor (DTR) depleter mice. As early as day 1 after Nb inoculation, CCR2+ monocytes were increased several fold in the lung and these high levels were sustained as late as day 7 after Nb inoculation, further evidence of significant recruitment of monocytes into the lung shortly after Nb inoculation (**Fig. 3c**). To further examine the extent to which monocytes contributed to the overall lung macrophage population after infection, $CCR2^{DTR}$ mice were inoculated with Nb and -1, 1, and 3 days later administered DT to deplete monocyte-derived macrophages. At 7 days after infection, NAMs were significantly reduced after DT administration (**Fig. 3d**) further corroborating a substantial contribution of monocytes to the NAM population. However, surprisingly, AMs also showed a marked reduction in their expansion typically observed after Nb inoculation (**Fig. 3e**). To confirm selective depletion of DT treatment on CCR2+ monocyte-derived macrophages, a separate myeloid population, eosinophils, which are $CCR2^{-}$, were also assessed. Eosinophils were also increased in the lung at 5 days after inoculation but were not affected by DT administration consistent with the specificity of the treatment (**Fig. 3f**). In aggregate, these data suggest that lung infiltrating monocytes acquire a tissue-resident phenotype and contribute to the increased AM population observed post-infection.

To corroborate and extend our congenic mouse transfer experiments, as well as our studies with the CCR2 depleter mice, we employed fate mapper mice that exploited characteristic CX3CR1 expression by monocytes[22]. With this mouse model, monocytes can be tracked in $^{Cx3cr1CreERT2\text{-}IRES\text{-}YFP}$ mice (abbreviated as Cx3cr1Cre mice), which express a tamoxifen (TAM)-inducible Cre recombinase (CreERT2) under the control of the endogenous *Cx3cr1* promoter, followed by an IRES–EYFP element. To track the fate of the Cx3cr1+ monocytes, Cx3cr1/Cre mice were crossed with *Rosa26*stop-tdTomato reporter mice (abbreviated as *R26*tdTomato mice), as previously described[22]. The resultant *Cx3*cr1$^{CreERT2\text{-}IRES\text{-}YFP/+}$Rosa26$^{floxed\text{-}tdTomato/+}$ mice were inoculated with Nb and administered TAM at two timepoints, day -1 and day +1 after infection, which

irreversibly labels CX3CR1$^+$ cells and their progeny by inducing the expression of tdTomato. At day 8 after inoculation, lung cell suspensions were collected and stained for markers associated with conventional AMs (CD64+,F4/80+,SiglecF+,CD11c+) (**Fig. 4a - 4c**). The gated AM subset was then analyzed for tdTomato expression. As shown in **Fig. 4d**, about 30% of AMs were tdTomato$^+$ post-Nb infection, indicating that these cells are derived from Cx3CR1+ monocytes. The use of these fate mapping mice obviated the need for cell transfers and/or generation of chimeras for tracing development of monocyte-derived AMs (Mo-AM), resulting in an actual analysis of Mo-AM differentiation under physiological conditions in the lung. Next, we sort-purified tissue-derived alveolar macrophages (TD-AM) (tdTomato-) and Mo-AMs (TdTomato+) and cultured them with Nb L3 to examine anti-helminth effector activity, as described above. As shown in Fig. **4e,f,** alveolar macrophages derived from CX3CR1+ monocytes were considerably more effective at impairing metabolic activity (decreased ATP) and killing L3 than their tissue-derived counterparts. These studies indicated that after Nb inoculation, monocytes enter the lung and transition to a general alveolar macrophage phenotype. However, they also develop unique characteristics, which include the capacity to preferentially damage and kill invading helminth larvae.

Our finding that these two alveolar macrophage lineages differed in terms of an anti-helminth macrophage phenotype raised the possibility that they may exhibit a more globally distinct activation phenotype. To address this, tdTomato+ MoAMs and tdTomato- TD-AMs were sort purified at day 7 after Nb inoculation and subjected to global transcriptome analyses. RNA-seq showed that at day 7 Mo-AMs macrophages had a gene expression profile distinct from TD-AMs while by day 14 the Mo-AMs had assumed gene expression profiles more similar to TD-AMs, as determined by pairwise Euclidean distance calculation (**Fig. 5a**) and principal components analysis (**Fig. 5b**). Visualization of overall expression patterns by volcano plots showed more transcriptonally regulated genes in Mo-AMs compared to TD-AMs at day 7 and day 14 (**Fig. 5c**). Venn diagrams of upregulated (Suppl. Fig. 1a) and downregulated (Suppl. Fig. 1b) further revealed the distinct differences in expressed genes between Mo-AMs and TD-AMs after Nb inoculation and canonical pathways analyses as revealed Ingenuity Pathway Analysis (IPA) further showed distinct differences (Suppl. Fig. 1c). . As canonical type 2 pathways (IPA analysis) were more pronounced in Mo-AMs relative to TD-AMs, and are critical in mediating helminth resistance, we directly compared gene expression of type 2 cytokines and markers at days 7 and 14 after Nb inoculation. As shown in the heat map in **Fig. 5d**, Arg 1, Retnla, IL-13, and Mgl2 were all increased in Mo-AMs relative to TD-AMs. At day 14, TD-AMs had returned to baseline levels or in some cases below levels observed in untreated TD-AMs. Thus, Mo-AMs contribute substantially to sustained increased levels of type 2 markers in AMs as late as day 14 after Nb inoculation. Notably, peroxisome proliferator-activated receptor gamma (PPARγ) associated signaling pathways, important in lipid metabolism and surfactant homeostasis[23], were instead significantly reduced in Mo-AMs relative to naïve Td-AMs at day 7 ($\log_2$ fold change -1.72) and day 14 ($\log_2$ fold change -1.95) after Nb inoculation. Analyses of in vivo proliferation of macrophage subsets showed similar levels of proliferation between TD-AMs and Mo-AMs at day 7 and day 14 after inoculation (**Suppl. Fig. 2a**). However, Seahorse real-time cell metabolic analyses revealed a higher oxygen consumption rate (OCR) and a higher extracellular

acidification rate (ECAR), in Mo-AMs compared to TD-AMs at day 7 after inoculation (**Suppl. Fig 2 b**), indicating increased oxidative phosphorylation and glycolysis respectively.

Although the macrophage-mediated mechanisms contributing to killing of parasitic nematode larvae remain unknown, several studies have now demonstrated that Arg1 activity is essential[3,7,8]. Our transcriptome RNAseq analyses revealed elevated levels of Arg1 gene expression in Mo-AMs, which were also most effective at killing L3. This was consistent with our findings that about 10% of total AMs expressed high levels of Arg 1(**Fig. 2c**). To corroborate these findings, we performed qPCR on tdTomato+ Mo-AMs and tdtomato- TD-AMs obtained from total lungs of *Cx3*cr1$^{\text{CreERT2-IRES-YFP/+}}$Rosa26$^{\text{floxed-tdTomato/+}}$ mice 8 days after L3 inoculation. As shown in **Fig. 6a**, Arg1 was preferentially expressed in tdTomato+ Mo-AMs. To assess whether Arg 1 protein was similarly increased in this subpopulation, tdTomato+ and tdTomato- alveolar macrophages were stained for intracellular Arg1 protein expression and analyzed by flow cytometric analysis. As shown in Fig. **6b,c**, Arg1 protein was expressed at considerably higher levels in FACS gated tdTomato^{+} Mo-AMs relative to tdTomato^{-} TD-AMs. These data suggest that despite the fact that Mo-AMs acquire similar phenotypes as TD-AMs, they maintain differential states of activation.

M2 macrophage activation is regulated by several factors including the production of type 2 cytokines by specialized innate immune cells. More specifically, our work and that of others have shown that neutrophils can contribute to M2 cell activation[3,6]. Therefore we sought to assess whether the high ARG1 expression was also dependent on Nb-activated neutrophils. A role for neutrophils in preferential activation of Mo-AMs would be consistent with a role for extrinsic signals as well as intrinsic cell lineage differences contributing to differential macrophage subset activation in the lung. To test this possibility, *Cx3*cr1$^{\text{CreERT2-IRES-YFP/+}}$Rosa26$^{\text{floxed-tdTomato/+}}$mice were administered TAM as described above and anti-Ly6g neutrophil depleting Ab or isotype control was administered at days -1, +1, and day 3 after Nb inoculation. At day 5 after inoculation total lung cell suspensions were stained for AMs and analyzed by flow cytometry for tdTomato expression. Elevations in intracellular Arg1 protein expression (Fig. 6d-f) and gene expression (Fig. 6g), as measured by RT-PCR, were significantly reduced in tdTomato+ Mo-AMs after neutrophil depletion.

The high Arg1 gene and protein expression in Mo-AMs and their enhanced capacity for helminth killing was consistent with Arg1 mediating helminth killing. Although the mechanism remains unclear, Arg1 triggers a cascade of effects resulting in production of potentially toxic urea and also polyamines, which can promote cellular activation and proliferation[17]. Recent studies have further shown an important role for Arg1 in depleting local arginine concentrations, and thereby attenuating activation of nearby immune cells, effectively resulting in immunosuppression[18]. Based on these latter findings, we hypothesized that one mechanism through which Arg1 may kill L3 would be through localized depletion of arginine, an essential amino acid for nematodes, as they are generally not thought to be capable of arginine biosynthesis[24,25]. To test this possibility, exsheathed L3 were cultured with bulk lung macrophages collected at day 5 after Nb inoculation as described above, but now increasing concentrations of arginine were added to potentially compensate for macrophage derived Arg1-mediated arginine depletion. As shown in **Fig. 7a**, as the arginine was increased, larval killing was

significantly decreased. Furthermore, live parasite metabolic activity, as measured by ATP values, markedly increased (**Fig. 7b**). To assess whether arginine was required for L3 survival under in vitro conditions, exsheathed larvae were cultured in arginine-free media. As shown in **Fig 7c**, parasite mortality was high in arginine-free media, while addition of arginine significantly reduced mortality. Corresponding increases in ATP by surviving L3 was further observed in arginine free media supplemented with exogenous arginine (**Fig. 7d**). Given these in vitro findings, we further hypothesized that administration of arginine in vivo could block macrophage-mediated helminth L3 killing. To test this possibility, lung macrophages were collected from donor BALB/c mice at day 7 after Nb inoculation and transferred to naïve recipient BALB/c mice. Two days later recipient mice were inoculated with Nb and supplemented with arginine in the drinking water. As shown in **Fig. 7e**, arginine supplementation markedly impaired primed macrophage mediated resistance, as evidenced by a significantly increased number of intestinal worms at day 5 after inoculation.

Discussion:

Macrophages mediate resistance to helminths as well as microbial pathogens. Recent studies suggest that the lung may be an important target for vaccine development against helminths[2], and that lung macrophages with anti-helminth effector functions develop shortly after Nb infection[3]. Tracking monocyte recruitment to the lungs and their differentiation in this microenvironment, we showed that during infection they can develop an alveolar macrophage-like phenotype that is distinct from TD-AMs and that preferentially mediates helminth killing and includes expression of high levels of Arg1. Development of this polarized Mo-AM phenotype was dependent on neutrophil help and our studies further show that macrophage-derived Arg.1 mediates parasite killing through localized depletion of arginine, providing a previously unappreciated nutrient deprivation mechanism for macrophage-mediated helminth killing.

Macrophages can exhibit plasticity in different tissue microenvironments developing characteristic phenotypes[15,22,26,27]. Here we show that monocytes recruited to the lung differentiate, within several days after parasite invasion, into an alveolar macrophage-like phenotype, but with distinct effector functions. Recent studies in a chimeric model showed that recruited Mo-Ams during influenza infection preferentially conferred protection against heterologous bacterial infections[15]. Interestingly, in an acute lung injury model fibrosis was also linked to a recruited Mo-AM population[16]. Our studies now show that tracking of monocytes, using fate mapping mice under physiological conditions, reveals their differentiation into Mo-AMs that are characterized by enhanced anti-helminth effector function and high Arg. 1 expression. Parasites typically leave the lung migrating to the small intestine by day 4 after inoculation[28]. The magnitude of the type 2 inflammatory response decreases shortly thereafter, but then levels off and a potent response is sustained thereafter resulting in chronic inflammation and development of emphysematous pathology[29]. Mo-AMs expressed high levels of CD11c and SiglecF by day 7 but transcriptome analyses revealed that they were distinct from TD-AMs as revealed by PCA and Euclidean distance analyses. The observation that this population expressed considerably higher levels of Arg1 and other type 2 markers compared to TD-AMs indicates a distinct activation state and effector function. By day 14, upregulated gene expression of immune response genes was decreased in the TD-AMs, while Mo-

AMs retained relatively high expression of these genes including type 2 markers. These findings are consistent with a model where TD-AMs revert back to a housekeeping phenotype shortly after infection, likely to assume their critical function of maintaining homeostasis and healthy lung function. In this context PPARγ expression remained higher in TD-AMs at both day 7 and day 14 after Nb inoculation relative to Mo-AMs. PPARγ mediates surfactant degradation, a critical homoestatic function of TD-AMs[23]. However, our findings may also be consistent with recent findings that AMs may undergo paralysis associated with poor phagocytic activity after bacterial infections[30]. Further studies of TD-AM function after helminth infection are needed to distinguish between these possibilities. In contrast alveolar macrophages derived from monocytes maintain a more activated phenotype with high expression of M2 markers, thus primed to respond to subsequent helminth infections. This primed state of Mo-AMs may also play a significant role in infections with heterologous pathogens, potentially providing protective immunity or alternatively increased susceptibility as has been observed with *Mycobacterium tuberculosis* infections[31]. As such, heterogeneity between individuals in innate and adaptive responses to specific pathogens may be potentially influenced by previous heterologous pathogen exposure.

Neutrophils are increasingly recognized as significant players in helminth infections and in cross talk with macrophages. Recent studies indicate that neutrophils exhibit a distinct alternatively activated (N2) phenotype during helminth infections[3] and that they can contribute resistance mechanisms leading to reduced worm burden after primary inoculation[4,5]. Interactions of macrophages with neutrophils can promote M2 activation, likely through both production of type 2 cytokines and direct cell-cell interactions involving efferocytosis[3,6]. Effects of neutrophil-macrophage crosstalk in driving activation and associated effector function of these myeloid cells can play a significant role in immune responses against diverse pathogens[32]. Our findings indicate that neutrophils are critical for the polarization of the monocyte-derived AM subset towards elevated expression of type 2 markers, including Arg1. Our findings that neutrophils preferentially stimulate this phenotype in recruited Mo-AMs indicates that both intrinsic lineage specific activation signatures and extrinsic signals provided in the lung tissue microenvironment interact to drive their activation culminating in an anti-helminth effector phenotype.

Although previous studies have identified Arg1 as being essential in macrophage-mediated helminth killing in the skin[7], lung[3], and small intestine[8], the mechanism through which this enzyme mediates this effect has remained unknown. Our studies now reveal a mechanism that is independent of the many molecules associated with the Arginase cascade culminating in production of urea, ornithine and polyamines. Instead out studies indicate that production of high levels of Arg1 by macrophages as they surround the invading parasitic larvae deprives the parasite of arginine. As we have now shown that arginine is required from external sources in Nb larval cultures, we now specifically show that Nb metabolism is slowed and mortality markedly increased in the absence of an external source of Arginine in Nb larval cultures. The developing L3 must thus likely obtain this essential amino acid from the vertebrate host as it traffics through various tissues. The ability of the activated M2 macrophage to rapidly adhere to and swarm around the invading L3 results in a localized depletion of this critical nutrient, effectively providing a potent anti-helminth effector mechanism. Our findings that arginine supplementation was sufficient to block macrophage-mediated killing in both in vitro cultures and in vivo

indicates the potent effect of the anti-helminth macrophage effector mechanism. Given the intense selection pressure of helminths on vertebrate evolution, one can postulate that the high level of Arg1 produced by M2 macrophages, specifically helminth activated Mo-AMs, may in part be an adaptation resulting in a potent resistance mechanism against these multicellular pathogens. It is intriguing that in microbial infections arginine also plays a critical role in resistance, through generation of nitric oxide synthase 2 activity resulting in production of anti-microbial nitric oxide. As such, arginine metabolism thus plays an important role in mediating resistance against eukaryotic as well as microbial pathogens although the mechanisms contributing to the protective response are quite different.

Fig. 1 Substantial changes in lung macrophage subsets occurs after N. brasiliensis inoculation.

Flow cytometric analysis of macrophage subsets obtained from single cell suspensions of whole lungs from Balb/c mice at days 1, 7, and 14 after *N. brasiliensis* inoculation. (a) Total numbers of lung macrophages (CD64+, F4/80^{+}, CD11c^{var}); (b) monocytes (CD11b^{+},Ly6C^{+}); (c) alveolar macrophages (AMs), (CD64+,F4/80+,SiglecF+,CD11c+); (d) Non-alveolar macrophages (NAMs) (CD64+,F4/80+,SiglecF^{-},CD11c^{var}); (e) eosinophils (F4/80+,SiglecF+, CD11c-). Each symbol represents an individual mouse with mean and SE shown. All results are representative of two independent experiments. *$p<0.05$, **$p<0.01$.

Fig. 2 Alveolar macrophages preferentially contribute to parasite killing and express high arginase.

(a, b) Lung alveolar macrophages (AMs) and nonalveolar macrophages (NAMs) were stained as in Fig. 1 and sort purified from whole lung cell suspensions at day 7 after *N. brasiliensis* inoculation of BALB/c mice. AMs and NAMs were seeded to 24-well plates (2 x 10^6 cell/well) and co-cultured with 200 exsheathed third stage larvae (L3). At day 5 after culture, the percent mortality (a) and worm ATP concentration (b) were determined. This experiment was repeated three times with similar results. (c, d) Representative flow cytometry plots (c) and lung macrophage numbers (d) for cytoplasmic arginase protein expression in AMs and NAMs at day 7 after *N. brasiliensis*-inoculation. Each symbol represents triplicates of pooled samples (a, b), or individual mice (d). All results are representative of two independent experiments. **$p<0.01$

Fig. 3 Lung infiltrating monocytes acquire a tissue-resident phenotype and contribute to the increased alveolar macrophage population after *N. brasiliensis* inoculation.

(a) At day 7 after *N. brasiliensis* (Nb) inoculation, donor macrophages including total macrophages, alveolar macrophages (AMs), and non-alveolar macrophages (NAMs) were electronically sorted and transferred to recipient mice, which were inoculated with Nb two days later. Recipient mice were assayed for intestinal worm number at day 5 after inoculation; a control group did not receive macrophages. (b) donor CD45.1 mice were inoculated with Nb and 7 days later, lung NAMs and AMs (as described in Fig. 1) were sort-purified, and transferred i.t. into naive recipients (CD45.2), which were inoculated with Nb 2 days later. Donor and recipient lung AM populations were assessed at day 5 after Nb inoculation. Flow cytometry plots were representative of 3 mice per group and 2 independent experiments. (c) CCR2-GFP reporter mice were assessed by flow

cytometric analysis for monocyte recruitment to total lungs at days 1 and 7 after Nb inoculation. (d-f) Monocytes were depleted by administration of DT at -1, +1, and +3 after Nb inoculation of CCR2-DTR mice. At day 5 after Nb inoculation, numbers of lung NAM (d), AM (e), and eosinophils (f) were determine by flow cytometric analysis. Each symbol represents an individual mouse and horizontal lines indicate the mean. All results are representative of two independent experiments. **$p<0.01$

Fig. 4. Monocyte-derived alveolar macrophages preferentially damage and kill *N. brasiliensis* L3.
(a-d) Fate-mapping of monocyte-derived macrophages recruited to the lung after *N. brasiliensis* infection. *s* mice were pulse administered tamoxifen at days -1 and +1 after *N. brasiliensis* (Nb) inoculation. Whole lung was collected at day 7 after inoculation and single cell suspensions stained for aleveolar macrophages (AMs) as described in Fig. 1. $F480^+$,$CD64^+$ lung macrophages were gated for expression of CD11c and SiglecF (b,c) and double positive cells were in turn gated for tdTomato expression (d). (e, f) Lung tdTomato + (tdT+ AM) monocyte- derived AMs and tdTomato- (tdT-AM) tissue-derived AMs were sort purified from Nb-primed *Cx3*cr1$^{\text{CreERT2-EYFP-IRES-YFP/+}}$Rosa26$^{\text{floxed-tdTomato/+}}$ reporter mice at day 7 post-infection. Macrophage subsets were seeded to 24-well plates (1×10^6 cell/well) and co-cultured with 100 exsheathed L3. At day 5 after culture, worm ATP concentration (e) and percent mortality (f) were determined. Triplicate samples were assayed from pools of 20 larva from each well for determination of ATP concentration. Each symbol represents mean of triplicate samples and this experiment was repeated three times with similar results.

Fig. 5 Monocyte-derived alveolar macrophages have distinct phenotype characterized by upregulation of type 2 markers.
*Cx3*cr1$^{\text{CreERT2-EYFP-IRES-YFP/+}}$Rosa26$^{\text{floxed-tdTomato/+}}$ reporter mice received tamoxifen at days -1, and +1 after *N. brasiliensis* (Nb) infection. At day 7 and day 14, tdTomato^+ monocyte-derived alveolar macrophages (mo-AMs) and TdTomato^- tissue-derived AMs (TD-AMs) were sorted-purified for RNA-seq transcriptional analysis and compared to naïve AMs, with 3 mice/treatment group. (a) pairwise Euclidean distance relative to the transcriptional profiles, demonstrating sample relatedness between AMs from untreated mice, and Mo-AMs and TD-AMs at day 7 and 14 after Nb inoculation (b) Principal Component Analysis of transcriptional profiles of treatment groups; (c) volcano plots of TD-AMs and Mo-AMs individual gene expression profiles at day 7 and day 14 expressed as compared to AMs from naïve mice; (d) Expression of selected characteristic type 2 response markers in TD-AMs and Mo-AMs at day 7 and day 14 after Nb inoculation as expressed relative to AMs from naïve mice(Log_2 fold change).
Fig. 6 After *N. brasiliensis* infection, monocyte-derived alveolar macrophages preferentially express arginase 1 which is dependent on extrinsic neutrophil signaling
(a-c) *Cx3*cr1$^{\text{CreERT2-EYFP-IRES-YFP/+}}$Rosa26$^{\text{floxed-tdTomato/+}}$ reporter mice were administered tamoxifen and inoculated with *N. brasiliensis* (Nb) as described in Fig. 5. (a) Arginase 1 (Arg1) mRNA levels by qPCR in subpopulations of lung alveolar macrophage (AM) subsets at day 8 after Nb inoculation expressed relative to naïve AMs; (b) Representative flow cytometric analysis of Arg1 intracellular protein expression in AM subsets at day 7 after Nb inoculation and (c) Arg 1 mean fluorescence intensity (MFI) in individual samples

from different treatment groups; (d-g) *Cx3*cr1$^{CreERT2\text{-}EYFP\text{-}IRES\text{-}YFP/+}$Rosa26$^{floxed\text{-}tdTomato/+}$ reporter mice were administered anti-Ly6G Ab or isotype control at days -1,1,and 3 and given tamoxifen at days -1 and 1 after Nb inoculation. (d-f) representative flow cytometric analyses of Arg1 intracellular protein expression after neutrophil depletion (f) Arg1 MFI in individual samples from each treatment group. (g) Arg1 mRNA levels by qPCR in macrophage subsets, presented as the fold increase over naïve AMs. Data shown are the mean and SEM of triplicate samples (a) or of duplicated samples (g) from a pool of four to eight mice per group and are representative of two independent experiments. Each symbol represents an individual mouse and horizontal lines indicate the mean. All results are representative of two independent experiments. *$p<0.05$, **$p<0.01$

Fig. 7 L-arginine is an essential amino acid nutrient for survival of *N. brasiliensis* larvae

(a, b) Total lung macrophages were sort-purified, as described in Fig. 1, at day 7 after *N. brasiliensis* (Nb) inoculation, seeded to 24-well plates (1 x 10^6 cell/well) and co-cultured with 100 exsheathed third stage larvae (L3) supplemented with L-arginine. At day 5 after culture, the percent mortality (**a**) and larval ATP concentration (**b**) were determined, as described in Fig. 4; this experiment was repeated three times with similar results. (c, d) ex-sheathed Nb larva (100 L3) were seeded to 12 well plates and cultured with L-arginine free RPMI1640 media, with one group supplemented with L-arginine. At day 3, 8, and 15 after culture, the percent mortality was assessed (**c**), and remaining worm ATP concentration assessed at day 15 (**d**). Data are presented as the mean and SEM of triplicate samples (c) or presented as individual samplse obtained from 20 larva from each well for determination of ATP concentration and horizontal lines indicate the mean(d). (e) At day 7 after Nb inoculation, donor macrophages were electronically sorted and transferred to recipient mice, which were inoculated with Nb two days later. Recipient mice were supplemented with 3% of L-arginine in drinking water starting at 7 days prior to Nb inoculation. Recipient mice were examined for intestinal worms at day 5 after inoculation and controls included mice not receiving macrophages, and not receiving macrophages but supplemented with L-arginine in drink water. Each symbol represents an individual mouse and horizontal lines indicate the mean. All results are representative of two independent experiments. *$p<0.05$, **$p<0.01$

Material and methods

Mice

BALB/c ByJ (CD45.1, cat#006584), BALB/c (CD45.2, cat#000651), *Rosa26*$^{\text{floxed-tdTomato}}$ and *Cx3cr1*$^{\text{CreERT2-IRES-YFP}}$ BL/6 mice were purchased from The Jackson Laboratory (Bar Harbor, ME). CCR2-DTR and CCR2-GFP Bl/6 mice were a kind gift from Dr. Amariliz – Medina (Center for Immunity and Inflammation, Rutgers university, NJ). All mice were maintained in a specific pathogen-free, virus Ab-free facility during the experiments. Healthy 8-12 week old mice were selected for treatment groups from purchased or bred colonies, without using specific randomization methods or specific blinding methods. The studies have been reviewed and approved by the Institutional Animal Care and Use Committee at Rutgers-the State University of New Jersey. The experiments herein were conducted according to the principles set forth in the Guide for the Care and Use of Laboratory Animals, Institute of Animal Resources, National Research Council, Department of Health, Education and Welfare (US National Institutes of Health).

Parasite culture and inoculation of mice

N. brasiliensis (NB) L3 were maintained in a petri dish culture containing charcoal and sphagnum moss. The larvae were isolated from cultures using a modified Baermann apparatus with 400U penicillin, 400 µg ml^{-1} streptomycin, and 400 µg ml^{-1} Neomycin (GIBCO, Rockville, MD) in sterile PBS, and then washed with sterile PBS three times. Mice were inoculated subcutaneously with a 40µl suspension of 650 Nb L3.

Flow cytometry, cell sorting, adoptive transfer

Lung tissue was washed with stirring at room temperature for 10 min in Hank's balanced salt solution (HBSS) with 1.3 mM EDTA (Invitrogen), then minced and treated at 37ºC for 30 min. with collagenase (1 mg / ml; Sigma) in RPMI1640 with 10% fetal calf serum (FCS) and with 100 µg / ml of DNase for 10 min. Cells were lysed with ACK (Lonza, Walkersville, MD) to remove erythrocytes. Cells were blocked with Fc Block (BD Biosciences, San Jose, CA), directly stained with fluorochrome-conjugated antibodies against CD45,F4/80, CD64, CD11c, Siglec-F,CD11b,Ly6C, and analyzed by flow cytometry. For adoptive transfer, macrophages (F4/80^{+}CD64^{+}SiglecF ^{vari}CD11c ^{vari}), alveolar macrophages (AMs) (F4/80^{+}CD64^{+}SiglecF^{+}CD11c ^{hi}), or nonalveolar macrophages (NAMs) (F4/80^{+}CD64^{+}SiglecF^{-}CD11c ^{vari}), were electronically sort purified (>98%), 5 million cells were transferred i.t. into recipient mice. Two days after cell transfer, the recipients were inoculated with Nb L3. In some experiments, L-arginine was added to the drinking water of recipients at day 7 before L3 inoculation.

For *Cx3cr1*$^{\text{CreERT2-IRES-YFP}}$ x *Rosa26*$^{\text{floxed-tdTomato}}$ reporter mice, single cells were isolated from whole lung and directly stained with fluorochrome-conjugated antibodies against CD45, F4/80, CD64, CD11c, Siglec-F and analyzed by flow cytometry. Cells were gated on CD45+,F4/80+,CD64+ cells, then further gated on Siglec-F+, CD11c^{hi} AMs. AMs were separated into tdTomato+ monocyte-derived alveolar macrophages (Mo-AMs) amd tdTomato- alveolar macrophages (TD-AMs).

Macrophage and larval co-cultures, or larvae culture in L-arginine free medium, and

larval ATP assay

Macrophages, alveolar macrophages, or nonalveolar macrophages, were electronically sorted from mice inoculated with Nb for 7 days, and placed on 12-well plates (1 x 10^6) in 2 ml of RPMI1640 medium with 10% of FBS, 400U penicillin, 400 µg/ml streptomycin, and 100 µg/ ml gentamycin. 100 µl of serum from the donor mice was also added to medium. One hundred ex-sheathed L3 larvae were added to each well. Cells and worms were co-cultured for 5 days at 37°C. The procedure to ex-sheath larvae included incubation of L3 with 6.7 mM sodium hypochlorite in PBS for 15 min. at room temperature, washing the L3 six times with sterile PBS containing 400U penicillin and 400 µg ml−1 streptomycin. In some experiments, the L3 were cultured in L-arginine free RPMI1640 without cells and in some group commercial L-arginine was added to the medium. The ATP levels for the L3 were performed according to the manufacturer's instructions. Briefly, 10 Nb L3 were collected with 100 µl of RPMI1640 medium and 100µl of the Celltiter-Glo Luminescent reagent (Promega, Madison, WI) was then added. The larvae were homogenized and incubated for five minutes at room temperature to stabilize the luminescence signal. After the homogenate was centrifuged at 1000g for 2 minutes, 100 µl of supernatant was applied to the luminometer to measure luminescence. As a negative control, larvae in RPMI1640 medium were treated in boiling water for five minutes and after cooling, the worms were homogenized with reagent. Dead larvae after incubation with macrophages were defined as non-motile, outstretched bodies, with non-refractive internal structures.

Cytokine gene expression by RT-PCR

For qPCR, RNA was extracted from lung tissue or sorted macrophages and reverse transcribed to cDNA. qPCR was done with Taqman (Life Technologies Corporation, Carlsbad, CA) kits and the Applied Biosystems 7500 Real-Time PCR System. All data were normalized to 18S ribosomal RNA, and the quantification of differences between treatment groups was calculated according to the manufacturer's instructions. Gene expression is presented as the fold increase over naïve WT controls.

RNA sequencing

Alveolar macrophages from *Cx3*cr1$^{\text{CreERT2-IRES-YFP/+}}$Rosa26$^{\text{floxed-tdTomato/+}}$ Nb- inoculated mice were sort-purified by gating on CD45+,CD64+,F4/80+,CD11c+,SiglecF+ AMs then sorted based on tdTomato expression, with TD-AMs being TdT- and Mo-AMs TdT+. Cells from a minimum of three biological replicates were sorted and pooled. The purity of all cell populations was 98% or greater. RNA was extracted using the RNeasy Plus Micro Kit (catalog no. 74034; QIAGEN). Illumina-compatible libraries were generated using the NEBNext Ultra II DNA Library Prep Kit for Illumina (catalog no. E7645S; New England BioLabs) and sequenced using an Illumina NovaSeq 6000 system in a paired-end 2x50-base pair (bp) reads configuration. Bulk RNA-seq analysis was performed in accordance with the nf-core RNA-seq guidelines v.1.4.2[33]. Briefly, the output reads were aligned to the GRCm38 (mm10) genome using STAR, followed by gene count generation using feature Counts and StringTie[34-36]. Read counts were normalized and compared between groups for differential gene expression using DESeq2 with significance cutoff at false discovery rate-adjusted $p<0.05$[37]. Determination of functional

pathways was performed using Ingenuity Pathway Analysis (IPA) on differentially expressed genes.

Seahorse Assay

*Cx3*cr1$^{CreERT2\text{-}IRES\text{-}YFP/+}$Rosa26$^{floxed\text{-}tdTomato/+}$ and CX3CR1-cre mice (control group) received tamoxifen at one day before and one day after Nb inoculation (-1, +1 day) and were sacrificed at day 7. Lung single cells were isolated and td tomato+ and td tomato- alveolar macrophages from reporters or alveolar macrophages from control group mice were sorted via flow cytometry. Alveolar macrophages (~75,000 cells/well) from each group were seeded into CellTak (Corning, # 354240) coated XFp plates in XF RPMI complete assay media, and incubated at 37°C without CO_2 for 45 minutes. The assay was run on a Seahorse XFp Extracellular Flux Analyzer with each group of AMs run in duplicate. After 20 cycles of basal measurement, Rotenone and Antimycin A (Seahorse XF Cell Mito Stress Kit), inhibitors of mitochondrial complex I and III, respectively, were injected into each well for a final concentration of 0.5 uM/well. Oxidative phosphorylation was measured by the oxygen consumption rate (OCAR; pmol/min) while glycolysis was measured by the extracellular acidification rate (ECAR; mpH/min) due to the accumulation of lactate or other metabolic acids and release of protons into the extracellular medium.

5-Ethynyl-2´-deoxyuridine (EdU) incorporation assay

*Cx3*cr1$^{CreERT2\text{-}IRES\text{-}YFP/+}$Rosa26$^{floxed\text{-}tdTomato/+}$ mice received tamoxifen at one day before and one day after Nb inoculation (-1, +1 day), and received Edu (5mg/ml, 100 ul, i.p.) every other day starting from one day before Nb inoculation ((-1, +1, +3, +5 day) and sacrificed at day 7. Control groups received tamoxifen and Edu but were not inoculated with Nb. Lung macrophages were stained with fluorochrome-conjugated antibodies against CD45, F4/80, CD64, CD11c, Siglec-F, then Edu incorporation was assessed using Click-iT Edu flow cytometry cell proliferation assay kit (ThermoFisher scientific, cat#C10424).

Statistical analysis

Data were analyzed using the statistical software program Prism 8 (GraphPad Software, Inc., La Jolla, CA) and are reported as means (± SEM). Differences between two groups were assessed by student's T-test, differences among multiple groups were assessed by one way ANOVA and individual comparisons were analyzed using Holm-Sidak test. Differences of $p < 0.05$ were considered statistically significant.

1. Gause, W.C., Wynn, T.A. & Allen, J.E. Type 2 immunity and wound healing: evolutionary refinement of adaptive immunity by helminths. *Nat Rev Immunol* **13**, 607-614 (2013).
2. Harvie, M.*, et al.* The lung is an important site for priming CD4 T-cell-mediated protective immunity against gastrointestinal helminth parasites. *Infect Immun* **78**, 3753-3762 (2010).

3. Chen, F.*, et al.* Neutrophils prime a long-lived effector macrophage phenotype that mediates accelerated helminth expulsion. *Nat Immunol* **15**, 938-946 (2014).
4. Bouchery, T.*, et al.* Hookworms Evade Host Immunity by Secreting a Deoxyribonuclease to Degrade Neutrophil Extracellular Traps. *Cell host & microbe* **27**, 277-289 e276 (2020).
5. Sutherland, T.E.*, et al.* Chitinase-like proteins promote IL-17-mediated neutrophilia in a tradeoff between nematode killing and host damage. *Nat Immunol* **15**, 1116-1125 (2014).
6. Bosurgi, L.*, et al.* Macrophage function in tissue repair and remodeling requires IL-4 or IL-13 with apoptotic cells. *Science* **356**, 1072-1076 (2017).
7. Obata-Ninomiya, K.*, et al.* The skin is an important bulwark of acquired immunity against intestinal helminths. *J Exp Med* (2013).
8. Anthony, R.M.*, et al.* Memory T(H)2 cells induce alternatively activated macrophages to mediate protection against nematode parasites. *Nat Med* **12**, 955-960 (2006).
9. Gause, W.C., Rothlin, C. & Loke, P. Heterogeneity in the initiation, development and function of type 2 immunity. *Nat Rev Immunol* (2020).
10. Scott, C.L., Henri, S. & Guilliams, M. Mononuclear phagocytes of the intestine, the skin, and the lung. *Immunol Rev* **262**, 9-24 (2014).
11. Gundra, U.M.*, et al.* Alternatively activated macrophages derived from monocytes and tissue macrophages are phenotypically and functionally distinct. *Blood* **123**, e110-122 (2014).
12. Jenkins, S.J.*, et al.* Local macrophage proliferation, rather than recruitment from the blood, is a signature of TH2 inflammation. *Science* **332**, 1284-1288 (2011).
13. Bleriot, C., Chakarov, S. & Ginhoux, F. Determinants of Resident Tissue Macrophage Identity and Function. *Immunity* **52**, 957-970 (2020).
14. Hussell, T. & Bell, T.J. Alveolar macrophages: plasticity in a tissue-specific context. *Nature reviews. Immunology* **14**, 81-93 (2014).
15. Aegerter, H.*, et al.* Influenza-induced monocyte-derived alveolar macrophages confer prolonged antibacterial protection. *Nat Immunol* **21**, 145-157 (2020).
16. Misharin, A.V.*, et al.* Monocyte-derived alveolar macrophages drive lung fibrosis and persist in the lung over the life span. *J Exp Med* **214**, 2387-2404 (2017).
17. Kreider, T., Anthony, R.M., Urban, J.F., Jr. & Gause, W.C. Alternatively activated macrophages in helminth infections. *Curr Opin Immunol* **19**, 448-453 (2007).
18. Pesce, J.T.*, et al.* Arginase-1-expressing macrophages suppress Th2 cytokine-driven inflammation and fibrosis. *PLoS Pathog* **5**, e1000371 (2009).
19. Chen, F.*, et al.* An essential role for TH2-type responses in limiting acute tissue damage during experimental helminth infection. *Nat Med* **18**, 260-266 (2012).
20. Katona, I.M., Urban, J.F., Jr. & Finkelman, F.D. The role of L3T4+ and Lyt-2+ T cells in the IgE response and immunity to Nippostrongylus brasiliensis. *J Immunol* **140**, 3206-3211 (1988).
21. Liu, Q.*, et al.* B cells have distinct roles in host protection against different nematode parasites. *J Immunol* **184**, 5213-5223 (2010).
22. Gundra, U.M.*, et al.* Vitamin A mediates conversion of monocyte-derived macrophages into tissue-resident macrophages during alternative activation. *Nat Immunol* **18**, 642-653 (2017).

23. Caputa, G., Castoldi, A. & Pearce, E.J. Metabolic adaptations of tissue-resident immune cells. *Nat Immunol* **20**, 793-801 (2019).
24. Tyagi, R., Rosa, B.A., Lewis, W.G. & Mitreva, M. Pan-phylum Comparison of Nematode Metabolic Potential. *PLoS Negl Trop Dis* **9**, e0003788 (2015).
25. Zecic, A., Dhondt, I. & Braeckman, B.P. The nutritional requirements of Caenorhabditis elegans. *Genes Nutr* **14**, 15 (2019).
26. Okabe, Y. & Medzhitov, R. Tissue biology perspective on macrophages. *Nat Immunol* **17**, 9-17 (2016).
27. Glass, C.K. & Natoli, G. Molecular control of activation and priming in macrophages. *Nat Immunol* **17**, 26-33 (2016).
28. Anthony, R.M., Rutitzky, L.I., Urban, J.F., Jr., Stadecker, M.J. & Gause, W.C. Protective immune mechanisms in helminth infection. *Nat Rev Immunol* **7**, 975-987 (2007).
29. Chen, F.*, et al.* B Cells Produce the Tissue-Protective Protein RELMalpha during Helminth Infection, which Inhibits IL-17 Expression and Limits Emphysema. *Cell Rep* **25**, 2775-2783 e2773 (2018).
30. Roquilly, A.*, et al.* Alveolar macrophages are epigenetically altered after inflammation, leading to long-term lung immunoparalysis. *Nat Immunol* **21**, 636-648 (2020).
31. Potian, J.A.*, et al.* Preexisting helminth infection induces inhibition of innate pulmonary anti-tuberculosis defense by engaging the IL-4 receptor pathway. *J Exp Med* **208**, 1863-1874 (2011).
32. Espinosa, V.*, et al.* Type III interferon is a critical regulator of innate antifungal immunity. *Sci Immunol* **2**(2017).
33. Ewels, P.A.*, et al.* The nf-core framework for community-curated bioinformatics pipelines. *Nature biotechnology* **38**, 276-278 (2020).
34. Liao, Y., Smyth, G.K. & Shi, W. featureCounts: an efficient general purpose program for assigning sequence reads to genomic features. *Bioinformatics* **30**, 923-930 (2014).
35. Pertea, M.*, et al.* StringTie enables improved reconstruction of a transcriptome from RNA-seq reads. *Nature biotechnology* **33**, 290-295 (2015).
36. Dobin, A.*, et al.* STAR: ultrafast universal RNA-seq aligner. *Bioinformatics* **29**, 15-21 (2013).
37. Love, M.I., Huber, W. & Anders, S. Moderated estimation of fold change and dispersion for RNA-seq data with DESeq2. *Genome biology* **15**, 550 (2014).

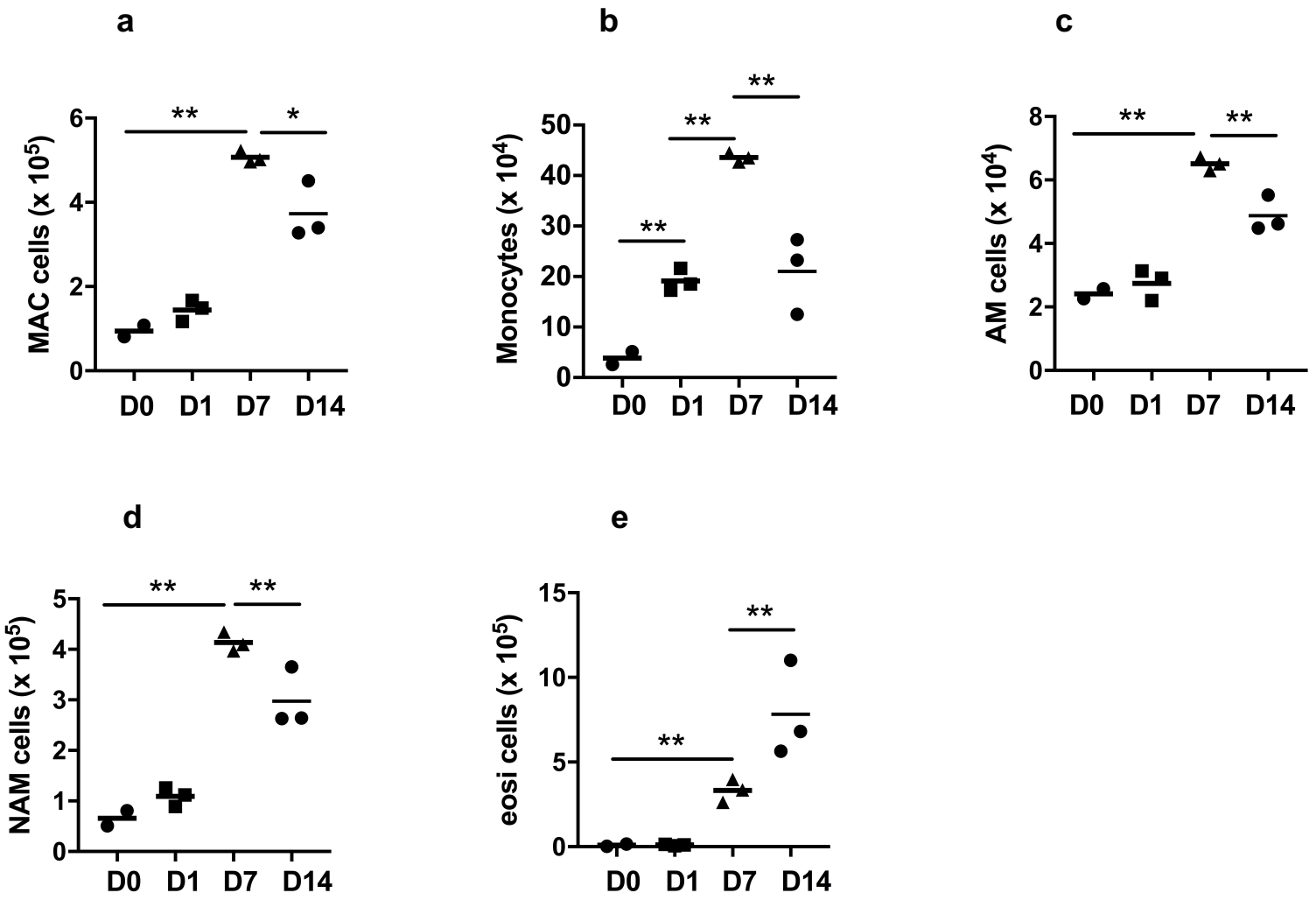
a
MAC cells (x 10^5)
0
2
4
6
**
*
D0
D1
D7
D14
b
Monocytes (x 10^4)
0
10
20
30
40
50
**
**
**
D0
D1
D7
D14
c
AM cells (x 10^4)
0
2
4
6
8
**
**
D0
D1
D7
D14
d
NAM cells (x 10^5)
0
1
2
3
4
5
**
**
D0
D1
D7
D14
e
eosi cells (x 10^5)
0
5
10
15
**
**
D0
D1
D7
D14

Fig. 1

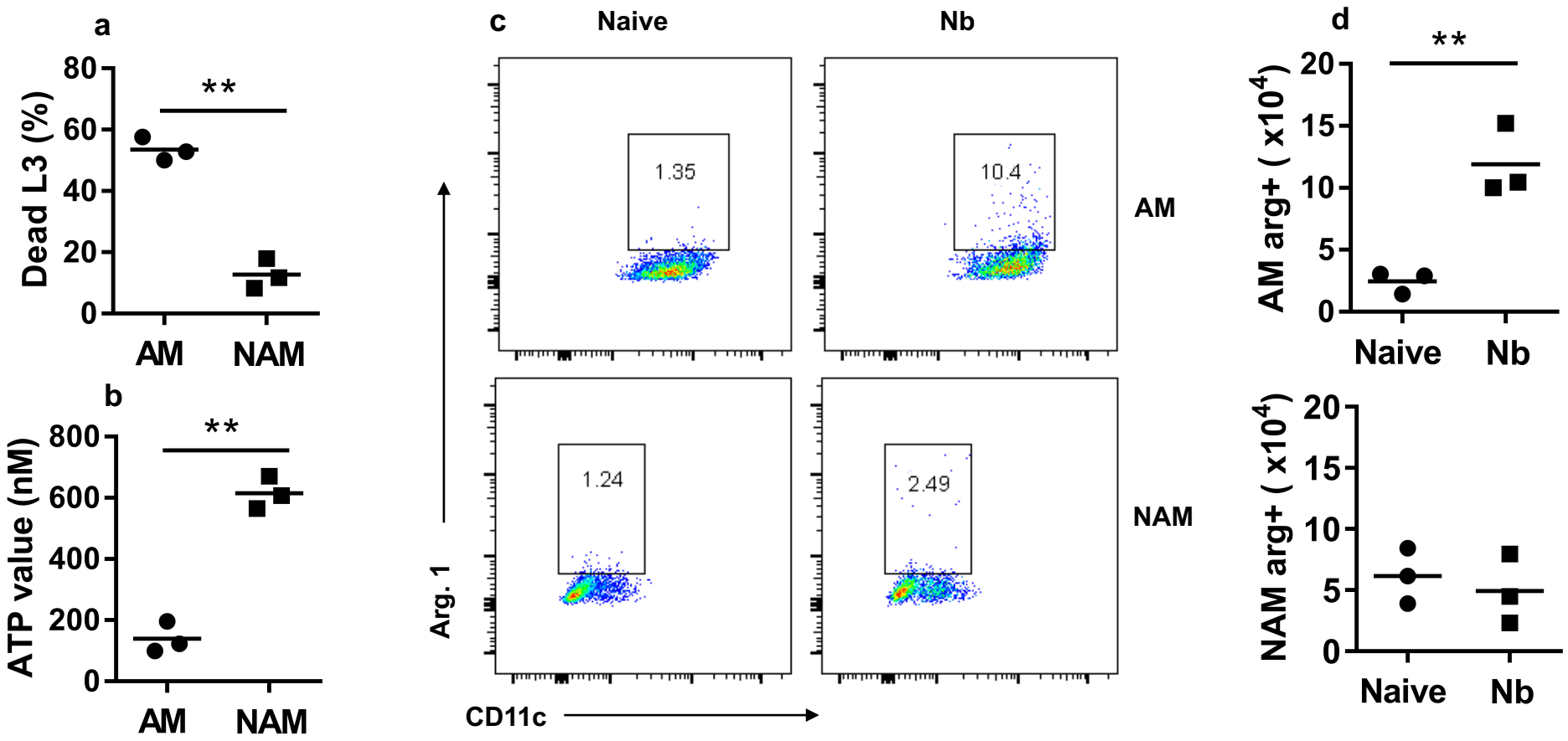
a
Dead L3 (%)
80
60
40
20
0
**
AM
NAM
b
ATP value (nM)
800
600
400
200
0
**
AM
NAM
c
Naive
Nb
1.35
10.4
AM
1.24
2.49
NAM
Arg. 1
CD11c
d
AM arg+ (x10^4)
20
15
10
5
0
**
Naive
Nb
NAM arg+ (x10^4)
20
15
10
5
0
Naive
Nb

Fig 2

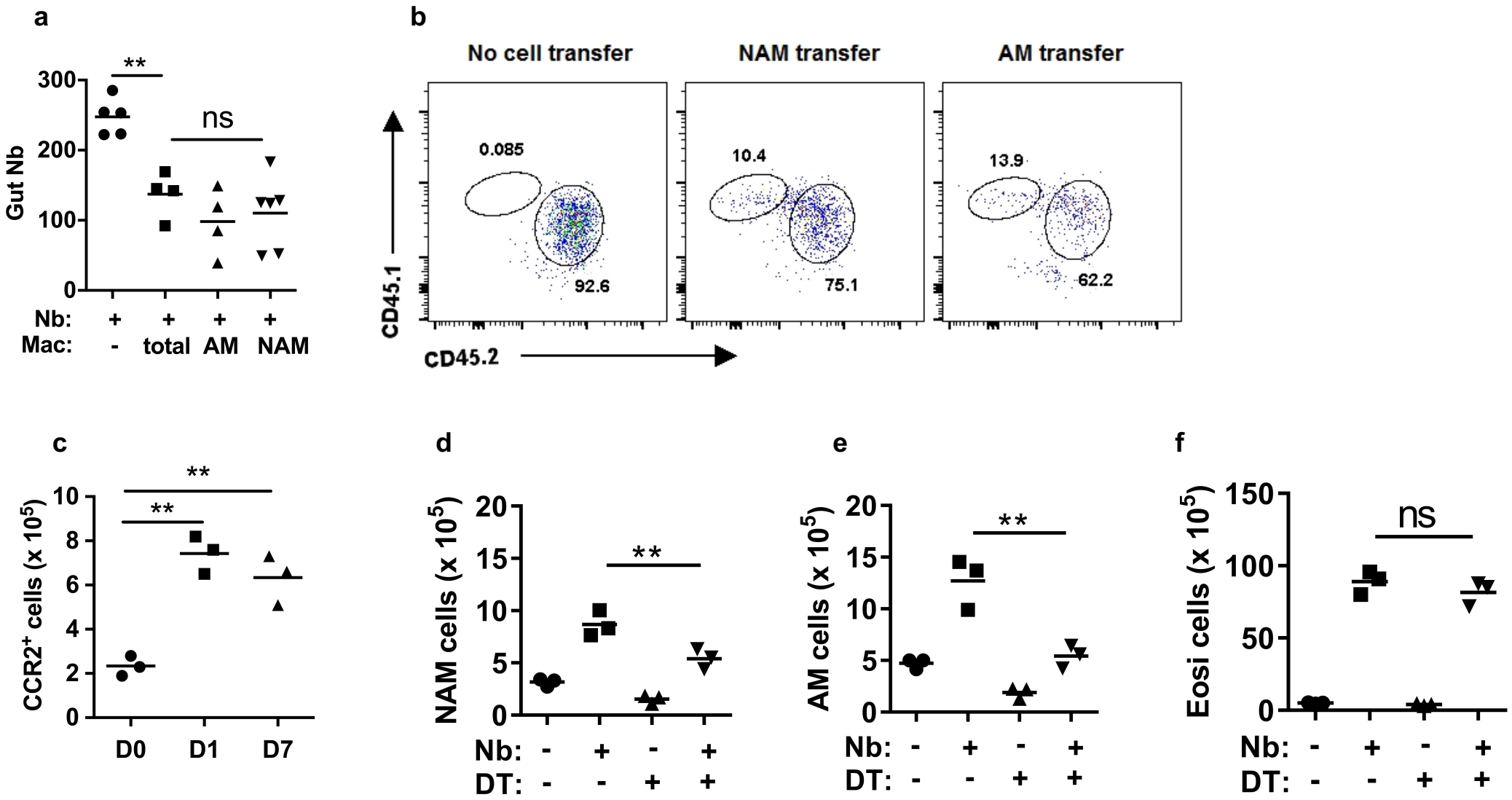
a
Gut Nb
300
200
100
0
**
ns
Nb: + + + +
Mac: - total AM NAM
b
No cell transfer
NAM transfer
AM transfer
0.085
92.6
10.4
75.1
13.9
62.2
CD45.1
CD45.2
c
CCR2+ cells (x 10^5)
10
8
6
4
2
0
**
**
D0
D1
D7
d
NAM cells (x 10^5)
20
15
10
5
0
**
Nb: - + - +
DT: - - + +
e
AM cells (x 10^5)
20
15
10
5
0
**
Nb: - + - +
DT: - - + +
f
Eosi cells (x 10^5)
150
100
50
0
ns
Nb: - + - +
DT: - - + +

Fig. 3

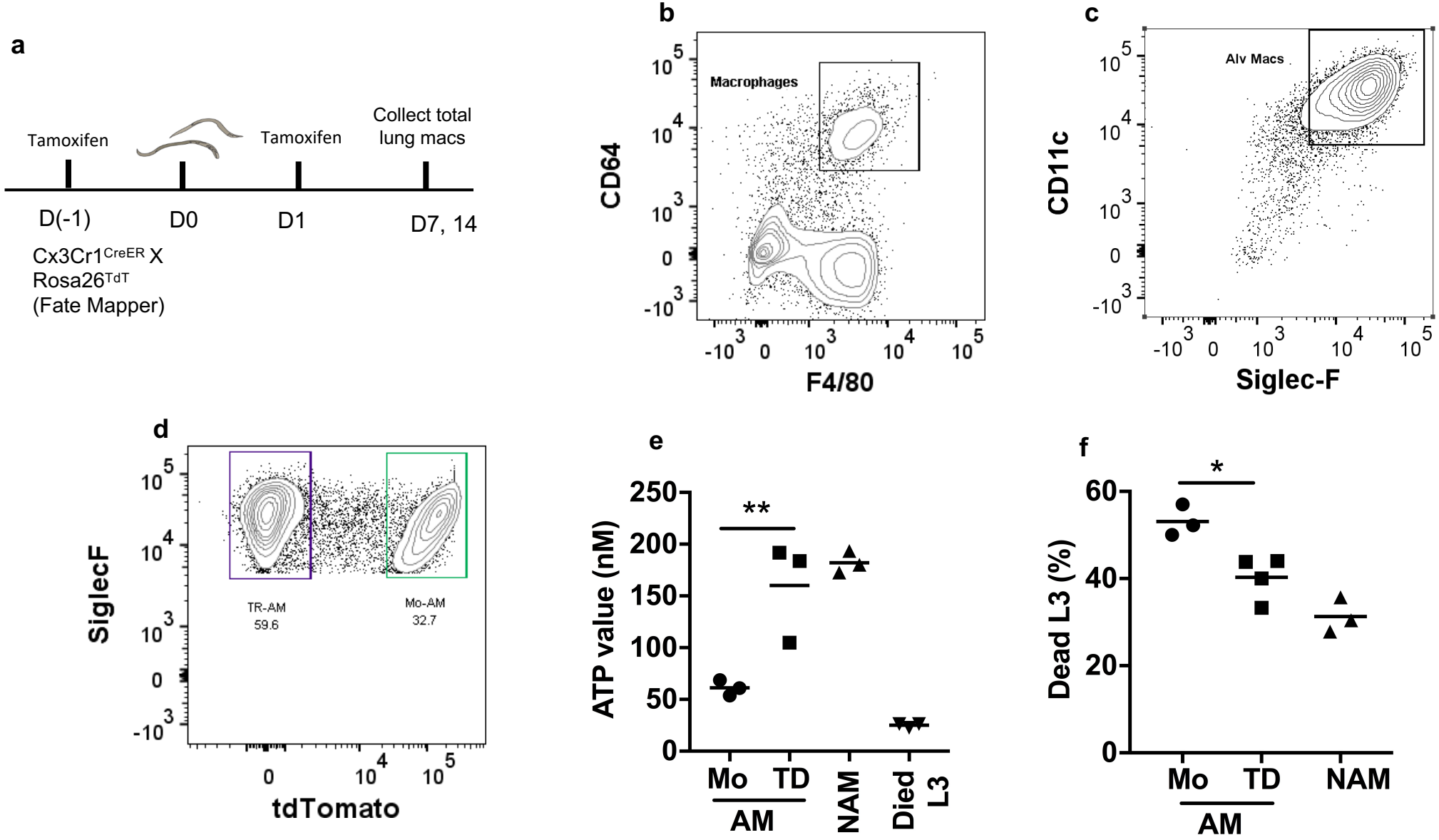
a
Tamoxifen
Tamoxifen
Collect total lung macs
D(-1)
D0
D1
D7, 14
Cx3Cr1CreER X
Rosa26TdT
(Fate Mapper)
b
Macrophages
CD64
F4/80
c
Alv Macs
CD11c
Siglec-F
d
TR-AM
59.6
Mo-AM
32.7
SiglecF
tdTomato
e
**
ATP value (nM)
Mo
TD
AM
NAM
Died L3
f
*
Dead L3 (%)
Mo
TD
AM
NAM

Fig. 4

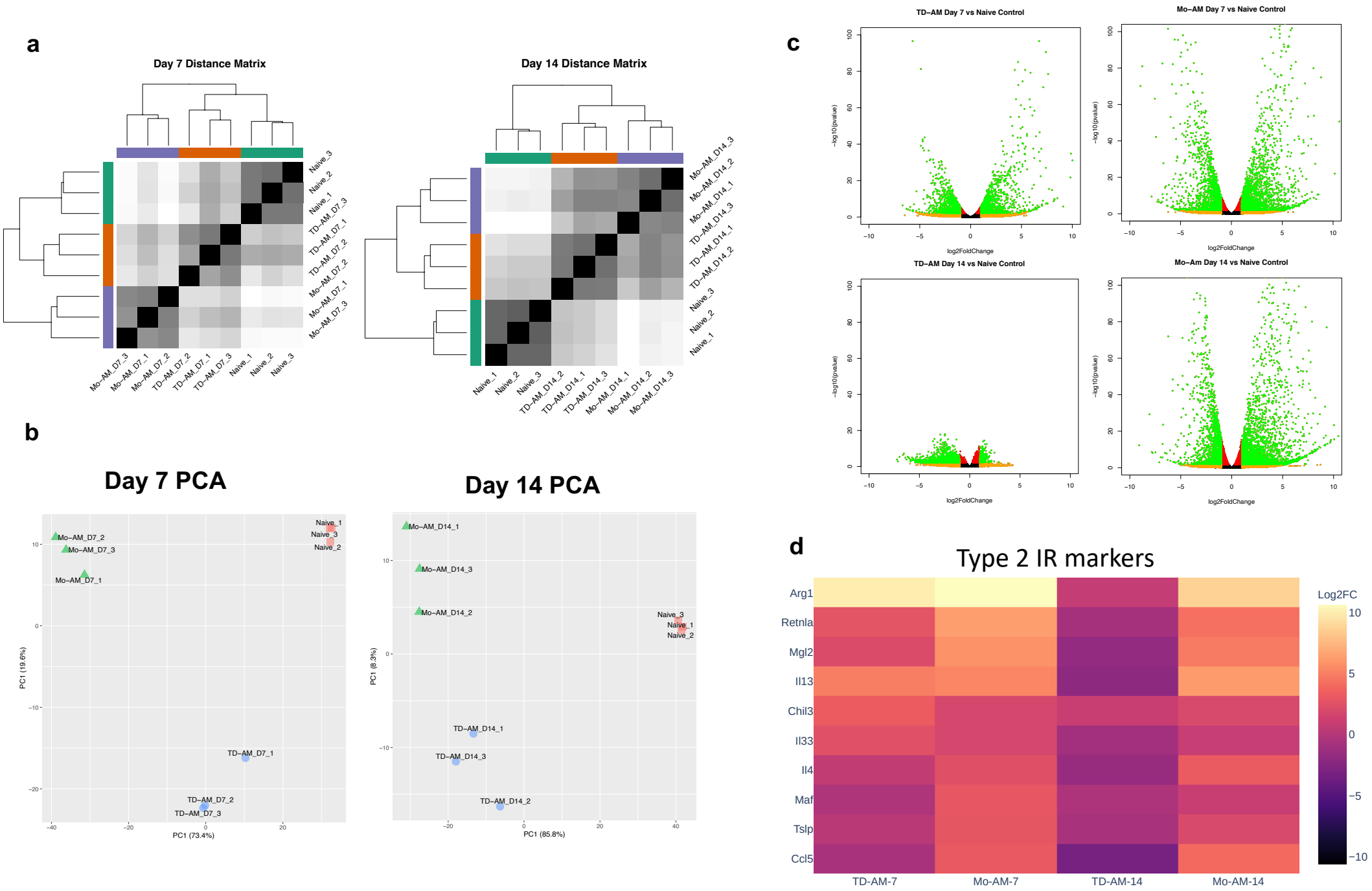
a
Day 7 Distance Matrix
Mo–AM_D7_3
Mo–AM_D7_1
Mo–AM_D7_2
TD–AM_D7_2
TD–AM_D7_1
TD–AM_D7_3
Naive_1
Naive_2
Naive_3
Day 14 Distance Matrix
Naive_1
Naive_2
Naive_3
TD–AM_D14_2
TD–AM_D14_1
TD–AM_D14_3
Mo–AM_D14_1
Mo–AM_D14_2
Mo–AM_D14_3
b
Day 7 PCA
PC1 (19.6%)
PC1 (73.4%)
Mo–AM_D7_2
Mo–AM_D7_3
Mo–AM_D7_1
Naive_1
Naive_3
Naive_2
TD–AM_D7_1
TD–AM_D7_2
TD–AM_D7_3
Day 14 PCA
PC1 (8.3%)
PC1 (85.8%)
Mo–AM_D14_1
Mo–AM_D14_3
Mo–AM_D14_2
Naive_3
Naive_1
Naive_2
TD–AM_D14_1
TD–AM_D14_3
TD–AM_D14_2
c
TD–AM Day 7 vs Naive Control
Mo–AM Day 7 vs Naive Control
TD–AM Day 14 vs Naive Control
Mo–Am Day 14 vs Naive Control
−log10(pvalue)
log2FoldChange
d
Type 2 IR markers
Arg1
Retnla
Mgl2
Il13
Chil3
Il33
Il4
Maf
Tslp
Ccl5
TD-AM-7
Mo-AM-7
TD-AM-14
Mo-AM-14
Log2FC
10
5
0
−5
−10

Fig. 5

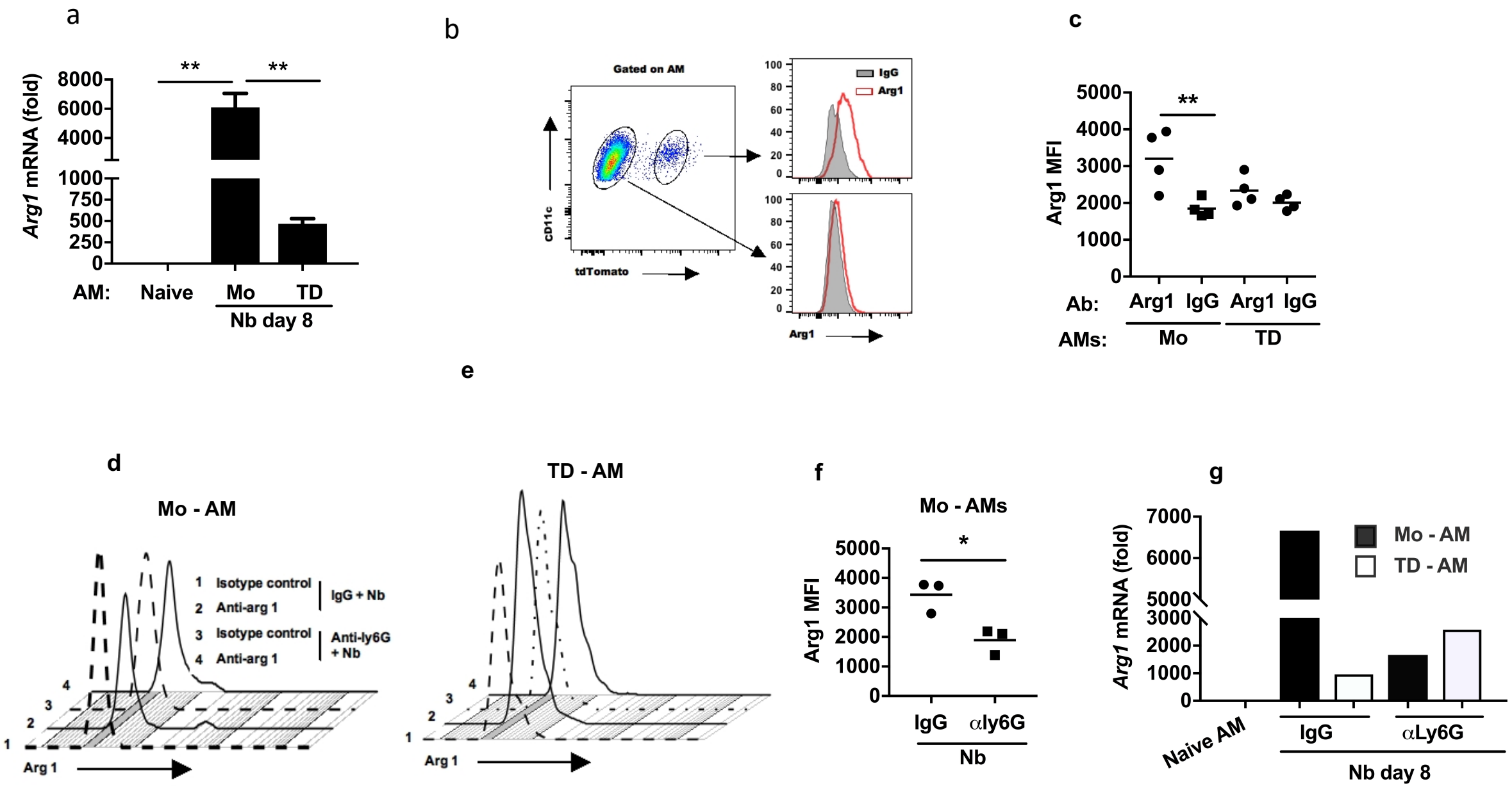
a
Arg1 mRNA (fold)
8000
6000
4000
1000
750
500
250
0
**
**
AM:
Naive
Mo
TD
Nb day 8
b
Gated on AM
cD11c
tdTomato
IgG
Arg1
Arg1
c
Arg1 MFI
5000
4000
3000
2000
1000
0
**
Ab:
Arg1
IgG
Arg1
IgG
AMs:
Mo
TD
d
Mo - AM
1 Isotype control
2 Anti-arg 1
IgG + Nb
3 Isotype control
4 Anti-arg 1
Anti-ly6G + Nb
Arg 1
e
TD - AM
Arg 1
f
Mo - AMs
Arg1 MFI
5000
4000
3000
2000
1000
0
*
IgG
αly6G
Nb
g
Arg1 mRNA (fold)
7000
6000
5000
3000
2000
1000
0
Mo - AM
TD - AM
Naive AM
IgG
αLy6G
Nb day 8

Fig. 6

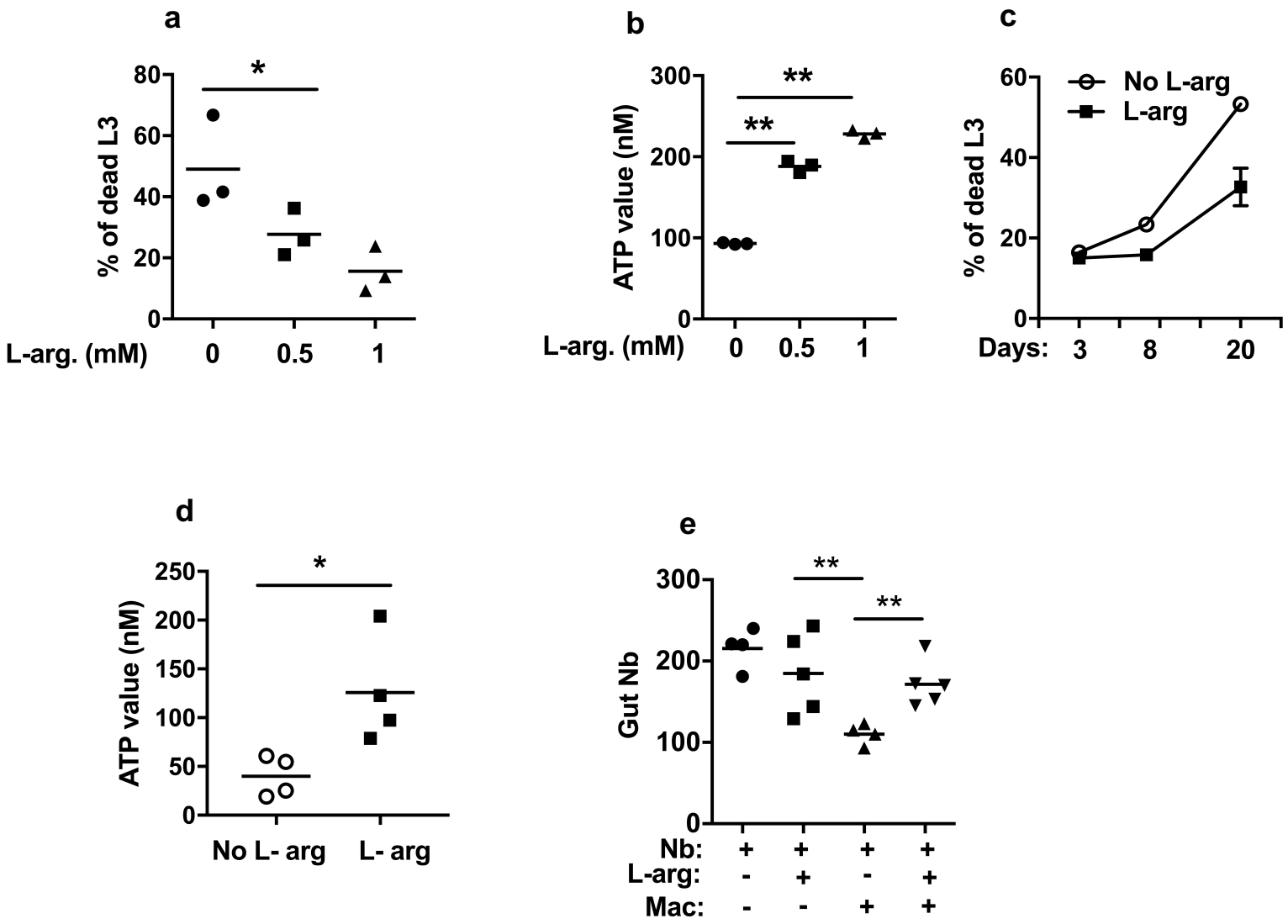
a
% of dead L3
80
60
40
20
0
*
L-arg. (mM)
0
0.5
1
b
ATP value (nM)
300
200
100
0
**
**
L-arg. (mM)
0
0.5
1
c
% of dead L3
60
40
20
0
No L-arg
L-arg
Days:
3
8
20
d
ATP value (nM)
250
200
150
100
50
0
*
No L- arg
L- arg
e
Gut Nb
300
200
100
0
**
**
Nb: + + + +
L-arg: - + - +
Mac: - - + +

Fig. 7